

RELATIVISTIC POYNTING JETS FROM ACCRETION DISKS

R. V. E. LOVELACE AND M. M. ROMANOVA

Department of Astronomy, Cornell University, 412 Space Science Building, Ithaca, NY 14853-6801;
 rv11@cornell.edu, romanova@astro.cornell.edu

Received 2003 May 5; accepted 2003 September 8; published 2003 September 30

ABSTRACT

A model is derived for relativistic Poynting jets from the inner region of a disk around a rotating black hole that is initially threaded by a dipole-like magnetic field. The model is derived from the special relativistic equation for a force-free electromagnetic field. The “head” of the Poynting jet is found to propagate outward with a velocity that may be relativistic. The Lorentz factor of the head is $\Gamma = [B_0^2/(8\pi\mathcal{R})^2\rho_{\text{ext}}c^2]^{1/6}$ if this quantity is much larger than unity. For conditions pertinent to an active galactic nuclei, $\Gamma \approx 8(10/\mathcal{R})^{1/3}(B_0/10^3 \text{ G})^{1/3}(n_{\text{ext}}/1 \text{ cm}^{-3})^{-1/6}$, where B_0 is the magnetic field strength close to the black hole, $\rho_{\text{ext}} = \bar{m}n_{\text{ext}}$ is the mass density of the ambient medium into which the jet propagates, $\mathcal{R} = r_0/r_g > 1$, where r_g is the gravitational radius of the black hole, and r_0 is the radius of the O-point of the initial dipole field. This model offers an explanation for the observed Lorentz factors of ~ 10 of parsec-scale radio jets measured with very long baseline interferometry.

Subject headings: galaxies: jets — galaxies: magnetic fields — galaxies: nuclei — quasars: general

1. INTRODUCTION

Highly collimated, oppositely directed jets are observed in active galaxies and quasars (see, e.g., Bridle & Eilek 1984 and Zensus, Taylor, & Wrobel 1998) and in old compact stars in binaries (Mirabel & Rodriguez 1994; Eikenberry et al. 1998). Furthermore, well-collimated emission-line jets are seen in young stellar objects (Mundt 1985; Bührke, Mundt, & Ray 1988). Recent work favors models for which the twisting of an ordered magnetic field threading an accretion disk acts to magnetically accelerate the jets (e.g., Meier, Koide, & Uchida 2001; Bisnovaty-Kogan & Lovelace 2001). There are two regimes: (1) the *hydromagnetic regime*, in which the energy and angular momentum are carried by both the electromagnetic field and the kinetic flux of matter, which is relevant to the jets from young stellar objects, and (2) the *Poynting flux regime*, in which the energy and angular momentum from the disk are carried predominantly by the electromagnetic field, which is relevant to extragalactic and microquasar jets and possibly to gamma-ray burst sources.

Different theoretical models have been proposed for magnetically dominated outflows and jets or Poynting outflows (Newman, Newman, & Lovelace 1992) and jets (Lynden-Bell 1996, 2003) from accretion disks threaded by a dipole-like magnetic field. Later, stationary Poynting flux–dominated outflows were found in axisymmetric magnetohydrodynamic (MHD) simulations of the opening of magnetic loops threading a Keplerian disk (Romanova et al. 1998). MHD simulations by Ustyugova et al. (2000) found collimated Poynting flux jets. The present work represents a continuation of the studies by Li et al. (2001) and Lovelace et al. (2002, hereafter L02), which are closely related to the work by Lynden-Bell (1996). Self-consistent force-free field solutions are obtained in which the twist of each field line is due to the differential rotation of a Keplerian disk.

2. THEORY OF POYNTING OUTFLOWS

Here we consider relativistic Poynting outflows from a rotating accretion disk around a Kerr black hole. We assume that at an initial time $t = 0$, an axisymmetric, dipole-like magnetic field threads the disk. The initial field geometry is shown in

the lower part of Figure 1. This field could result from dynamo processes in the disk (e.g., Colgate, Li, & Pariev 2001). A more general magnetic field threading the disk would consist of multiple loops going from radii, say, r_a to $r_b > r_a$ and from $r_c > r_b$ to $r_d > r_c$, etc. It is not clear how to treat this case analytically, but nonrelativistic MHD simulations of this type of field show strong Poynting flux outflows (Romanova et al. 1998).

The disk is assumed to be highly conducting and dense in the sense that $\rho_d(r\Omega)^2 \gg B^2/4\pi$, where ρ_d is the density and $\Omega(r)$ is the angular rotation rate of the disk. Thus, a magnetic field threading the disk is frozen into the disk. Furthermore, we suppose that the radial accretion speed of the disk is much smaller than the azimuthal velocity Ωr . For a corotating disk around a Kerr black hole,

$$\Omega = \frac{c^3/(GM)}{a_* + (r/r_g)^{3/2}}, \quad (1)$$

for $r > r_{\text{isco}}$, where r_{isco} is the innermost stable circular orbit. Here a_* is the spin parameter of the black hole with $0 \leq a_* < 1$, and $r_g \equiv GM/c^2$. For example, for $a_* = 0.99$, $r_{\text{isco}} \approx 1.45r_g$. The simplification is made that equation (1) also applies to $r < r_{\text{isco}}$. The region $r \leq r_{\text{isco}}$ has a negligible influence on our results for the considered conditions in which the radial scale of the magnetic field r_0 is such that $(r_g/r_0)^2 \ll 1$.

In the space above (and below) the disk, we assume a “coronal” or “force-free” ideal plasma (Gold & Hoyle 1960). This plasma may be relativistic, with a flow speed v comparable to the speed of light. Away from the head of the jet, the electromagnetic field is *quasi-stationary*. This limit is applicable under conditions in which the energy density of the plasma $\gamma\rho c^2$ is much less than the electromagnetic field energy density $(E^2 + B^2)/8\pi$.

Cylindrical (r, ϕ, z) -coordinates are used, and axisymmetry is assumed. Thus, the magnetic field has the form $\mathbf{B} = B_p \hat{\phi} + B_r \hat{r} + B_z \hat{z}$. We can write $B_r = -(1/r)(\partial\Psi/\partial z)$ and $B_z = (1/r)(\partial\Psi/\partial r)$, where $\Psi(r, z) \equiv rA_\phi(r, z)$ is the flux function. In the plane of the disk, the flux function is inde-

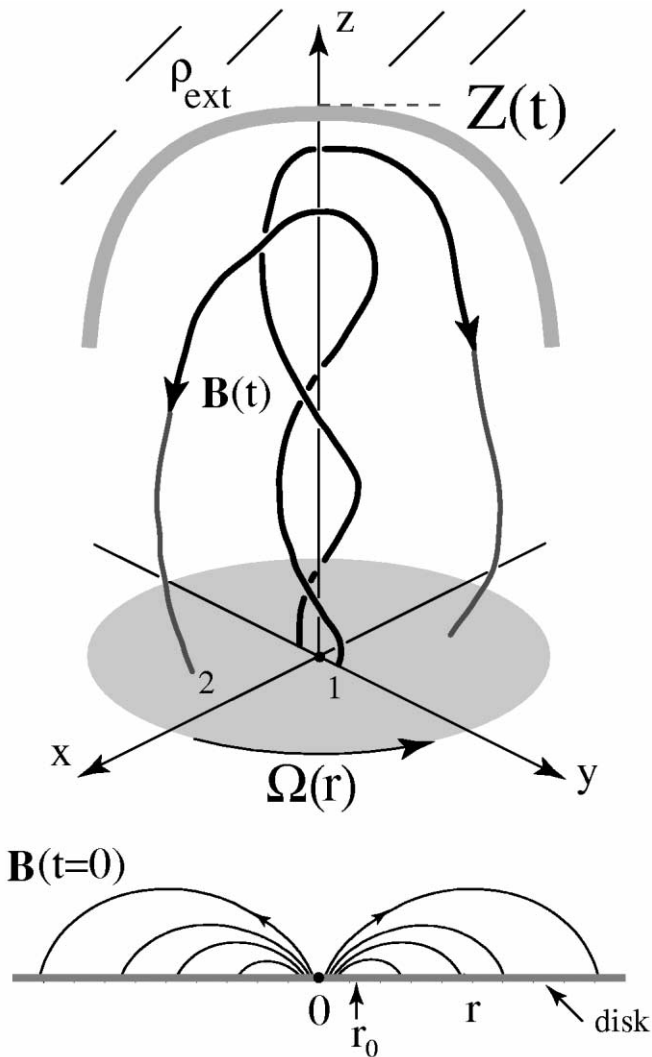


FIG. 1.—Sketch of the magnetic field configuration of a Poynting jet. The bottom part of the figure shows the initial dipole-like magnetic field threading the disk that rotates at an angular rate $\Omega(r)$. The top part of the figure shows the jet at some later time when the head of the jet is at a distance $Z(t)$. At the head of the jet, there is a force balance between the electromagnetic stress of the jet and the ram pressure of the ambient medium of density ρ_{ext} .

pendent of time owing to the frozen-in condition. A representative form of this function is

$$\Psi(r, 0) = \frac{1}{2} \frac{r^2 B_0}{1 + 2(r/r_0)^3}, \quad (2)$$

where B_0 is the axial magnetic field strength in the center of the disk and r_0 is the radius of the O-point of the magnetic field in the plane of the disk as indicated in Figure 1. Equation (2) is taken to apply to $r \geq 0$ even though it is not valid near the horizon of the black hole. As already mentioned, the contribution from this region is negligible for the considered conditions where $(r_g/r_0)^2 \ll 1$. Note that $\Psi(r, 0)$ has a maximum value of $r_0^2 B_0/6$ at the O-point where $\mathbf{B}(r_0, 0) = 0$. For $(r/r_0)^2 \ll 1$, $\Psi(r, 0) \propto r^2$, which corresponds to a uniform vertical field, whereas for $(r/r_0)^2 \gg 1$, $\Psi(r, 0) \propto 1/r$, which corresponds to the dipole field $B_z(r, 0) \propto -1/r^3$.

It is clear that equations (1) and (2) can be combined to give $\Omega = \Omega(\Psi)$, which is a double-valued function of Ψ . The upper

branch of the function is for the inner part of the disk ($r \leq r_0$), while the lower part is for the outer part of the disk. A good approximation for the upper branch is obtained by taking $\Psi \approx r^2 B_0/2$, which gives $\Omega = (c^3/GM)/[a_* + (2\Psi/B_0 r_g^2)^{3/4}]$.

The main equations for the plasma follow from the continuity equation $\nabla \cdot (\rho \mathbf{v}) = 0$, Ampère's law $\nabla \times \mathbf{B} = 4\pi \mathbf{J}/c$, Coulomb's law $\nabla \cdot \mathbf{E} = 4\pi \rho_e$, with ρ_e being the charge density, Faraday's law $\nabla \times \mathbf{E} = 0$, perfect conductivity $\mathbf{E} + \mathbf{v} \times \mathbf{B}/c = 0$, with \mathbf{v} being the plasma flow velocity, and the “force-free” condition in the Euler equation, $\rho_e \mathbf{E} + \mathbf{J} \times \mathbf{B}/c = 0$ (see, e.g., Lovelace, Wang, & Sulkanen 1987). Owing to the assumed axisymmetry, $E_\phi = 0$, so that the poloidal velocity $\mathbf{v}_p = \kappa \mathbf{B}_p$. Mass conservation then gives $\mathbf{B} \cdot \nabla(\rho \kappa) = 0$, which implies that $\rho \kappa = F(\Psi)/4\pi$, where F is an arbitrary function of Ψ . In a similar way, one finds that $v_\phi - \kappa B_\phi = rG(\Psi)$, so that $\mathbf{E} = -G(\Psi)\nabla\Psi$, and $rB_\phi = H(\Psi)$, so that there are two additional functions, G and H .

The function G is determined along all of the field lines that go through the disk. This follows from the perfect conductivity condition at the surface of the disk, $z = 0$, $E_r + (\mathbf{v} \times \mathbf{B})_r/c = 0$. This gives $E_r = -(v_\phi B_z - v_z B_\phi)/c = -v_\phi B_z/c$, where v_z is zero at the disk and v_ϕ is the disk velocity. Therefore, $E_r(r, 0) = -\Omega[d\Psi(r, 0)/dr]/c$, so that $G(\Psi) = \Omega(r)/c$, which gives $\Omega = \Omega(\Psi)$.

The component of the Euler equation in the direction of $\nabla\Psi$ gives the force-free Grad-Shafranov equation

$$\left[1 - \left(\frac{r\Omega}{c}\right)^2\right] \Delta^* \Psi - \frac{\nabla\Psi}{2r^2} \cdot \nabla \left(\frac{r^4 \Omega^2}{c^2}\right) + HH' = 0, \quad (3)$$

with $\Delta^* \equiv \partial^2/\partial r^2 - (1/r)(\partial/\partial r) + \partial^2/\partial z^2$ and $H' = dH(\Psi)/d\Psi$ (Scharlemann & Wagoner 1973; Lovelace et al. 1987).

As mentioned above, we consider an *initial value problem* in which the disk at $t = 0$ is threaded by a dipole-like poloidal magnetic field. The form of $H(\Psi)$ in equation (3) is then determined by the differential rotation of the disk: the azimuthal *twist* of a given field line going from an inner footpoint at r_1 to an outer footpoint at r_2 is fixed by the differential rotation of the disk.

Ampère's law gives $\oint d\mathbf{l} \cdot \mathbf{B} = (4\pi/c) \int dS \cdot \mathbf{J}$, so that $rB_\phi(r, z) = H(\Psi)$ is $(2/c)$ times the current flowing through a circular area of radius r (with normal \hat{z}) labeled $\Psi(r, z) = \text{const}$. Equivalently, $-H[\Psi(r, 0)]$ is $(2/c)$ times the current flowing into the area of the disk $\leq r$. Our previous work (Li et al. 2000; L02) shows that $-H(\Psi)$ has a maximum value, so that the total current flowing into the disk for $r \leq r_m$ is $I_{\text{tot}} = (c/2)(-H)_{\text{max}}$, where r_m is such that $-H[\Psi(r_m, 0)] = (-H)_{\text{max}}$ (where r_m is less than the radius of the O-point, r_0). The same total current I_{tot} flows out of the region of the disk $r = r_m$ to r_0 .

For a given field line, we have $r d\phi/B_\phi = ds_p/B_p$, where $ds_p \equiv (dr^2 + dz^2)^{1/2}$ is the poloidal arc length along the field line and $B_p \equiv (B_r^2 + B_z^2)^{1/2}$. The total twist of a field line loop is

$$\Delta\phi(\Psi) = - \int_1^2 ds_p \frac{B_\phi}{rB_p} = -H(\Psi) \int_1^2 \frac{ds_p}{r^2 B_p}, \quad (4)$$

with the sign included to give $\Delta\phi > 0$. The integration goes from the disk at a radius $r_1 < r_0$ out into the corona and back to the disk at a radius $r_2 > r_0$. For a prograde disk, the field line twist after a time t is $\Delta\phi(\Psi) = \Omega(r_0)t\{[\Omega(r_1)/\Omega(r_0)] - [\Omega(r_2)/\Omega(r_0)]\}$.

2.1. Poynting Jets

Our previous study of nonrelativistic Poynting jets by analytic theory (L02) and axisymmetric MHD simulations (Ustyugova et al. 2000) showed that as the twist, as measured by $\Omega(r_0)t$, increases, a new, high twist field configuration appears with a different topology. A ‘‘plasmoid’’ consisting of toroidal flux detaches from the disk and propagates outward. The plasmoid is bounded by a poloidal field line that has an X-point above the O-point on the disk. The occurrence of the X-point requires that there be at least a small amount of dissipation in the evolution from the poloidal dipole field and the Poynting jet configuration. The high-twist configuration consists of a region near the axis that is *magnetically collimated* by the toroidal B_ϕ field and a region far from the axis that is *anti-collimated* in the sense that it is pushed away from the axis. The field lines returning to the disk at $r > r_0$ are anticollimated by the pressure of the toroidal magnetic field. The *poloidal field* fills only a small part of the coronal space.

In the case of relativistic Poynting jets, we hypothesize that the magnetic field configuration is similar to that in the non-relativistic limit (L02; Ustyugova et al. 2000). Thus, most of the twist $\Delta\phi$ of a field line of the relativistic Poynting jet occurs along the jet from $z = 0$ to $Z(t)$ as sketched in Figure 1, where $Z(t)$ is the axial location of the ‘‘head’’ of the jet. Along most of the distance $z = 0 - Z$, the radius of the jet is a constant, and $\Psi = \Psi(r)$ for $Z \gg r_0$. Note that the function $\Psi(r)$ is different from $\Psi(r, 0)$, which is the flux function profile on the disk surface. Hence, $r^2 d\phi/dz = rB_\phi(r, z)/B_z(r, z)$. We take for simplicity that $V_z = dZ/dt = \text{const}$. We determine V_z in § 3. In this case, $H(\Psi) = [r^2\Omega(\Psi)/V_z]B_z$, where the right-hand side can be written as a function of Ψ and $d\Psi/dr$. This relation allows the closure of equation (3), which can now be written as

$$\frac{d^2\Psi}{dr^2} + \frac{\lambda - 1}{\lambda + 1} \frac{1}{r} \frac{d\Psi}{dr} + \frac{\lambda}{\lambda + 1} \left(\frac{d\Psi}{dr}\right)^2 \frac{1}{\Omega} \frac{d\Omega}{d\Psi} = 0, \quad (5)$$

where $\lambda \equiv (r\Omega/c)^2[(c/V_z)^2 - 1] = (r\Omega/c)^2/(\Gamma^2 - 1)$, with $\Gamma \equiv 1/(1 - V_z^2/c^2)^{1/2}$.

The solution to equation (5) is facilitated by introducing dimensionless variables. We measure the radial distance in units of the distance r_0 to the O-point of the magnetic field threading the disk (eq. [2]). We measure the flux function Ψ in units of $\Psi_0 \equiv r_0^2 B_0/2$. The fields are measured in units of B_0 , which is the magnetic field strength at the center of the disk. Thus, $\bar{B}_z = (2\bar{r})^{-1} d\Psi/d\bar{r}$. The disk rotation rate Ω is measured in units of $c^3/(GM)$ (eq. [1]). In terms of the dimensionless variables \bar{r} , $\bar{\Psi}$, and $\bar{\Omega}$, equation (5) is the same, but with the overbars on these three variables. Note also that $\lambda = \bar{r}^2 \bar{\mathcal{R}}^2 \bar{\Omega}^2 / (\Gamma^2 - 1)$, where $\bar{\mathcal{R}}^2 \equiv (r_0/r_g)^2 \gg 1$.

We consider solutions to equation (5) using the approximation to equation (2) of $\Psi(r, 0) = \bar{r}^2$, which gives $\bar{\Omega} = 1/(a_* + \bar{\mathcal{R}}^{3/2} \bar{\Psi}^{3/4})$. These solutions are close to those obtained using the full dependence $\Omega(\Psi)$. We then have $\bar{\Omega} = 1/(a_* + \bar{\mathcal{R}}^{3/2} \bar{\Psi}^{3/4})$. In this approximation, there is a unique self-similar solution to equation (5) for $\bar{\Psi} \gg 1/\bar{\mathcal{R}}^2$, where $\bar{\Omega} \approx \bar{\mathcal{R}}^{-3/2} \bar{\Psi}^{-3/4}$. This solution is $\bar{\Psi} = \bar{r}^{4/3}/[2\bar{\mathcal{R}}(\Gamma^2 - 1)]^{2/3}$, with $\lambda = 2$. The dependence on r is the same as found in the nonrelativistic case by L02. The dependence holds for $\bar{r}_1 = [2(\Gamma^2 - 1)]^{1/2}/\bar{\mathcal{R}} < \bar{r} < \bar{r}_2 = [2(\Gamma^2 - 1)]^{1/2} \bar{\mathcal{R}}^{1/2}/3^{3/4}$. At the inner radius \bar{r}_1 , $\bar{\Psi} = 1/\bar{\mathcal{R}}^2$, which corresponds to the streamline that passes through the disk at a distance $r = r_g$. For $\bar{r} < \bar{r}_1$, we assume $\bar{\Psi} \propto \bar{r}^2$, which corresponds to $B_z = \text{const}$. At the outer radius \bar{r}_2 , $\bar{\Psi} = (\bar{\Psi})_{\text{max}} = \frac{1}{3}$, which cor-

responds to the streamline that goes through the disk near the O-point at $r = r_0$. Note that there is an appreciable range of radii if $\bar{\mathcal{R}}^{3/2} \gg 1$. The nonzero field components of the Poynting jet are $\bar{E}_r = -\sqrt{2}(\Gamma^2 - 1)^{1/2} \bar{B}_z$, $\bar{B}_\phi = -\sqrt{2}\Gamma \bar{B}_z$, and $\bar{B}_z = \frac{2}{3}(\bar{r}^{-2/3})/[2\bar{\mathcal{R}}(\Gamma^2 - 1)]^{2/3}$, which hold for $r_1 < r < r_2$. This electromagnetic field satisfies the radial force balance equation, $dB_z^2/dr + (1/r^2)d[r^2(B_\phi^2 - E_r^2)]/dr = 0$, as it should. At the outer radius of the jet at r_2 , there is a boundary layer where the axial field changes from $\bar{B}_z(r_2)$ to zero while (minus) the toroidal field increases by a corresponding amount so as to give the radial force balance. This gives $-r_2 B_\phi(r_2) = (-H)_{\text{max}} = 2I_{\text{max}}/c = (2/\sqrt{3})\Psi(r_2)/r_2$, which is close to the relation found in the non-relativistic case (L02).

3. FORCE BALANCE AT THE HEAD OF THE JET

In the rest frame of the central object, the axial momentum flux density is T_{zz} , where T_{jk} ($j, k = 0, 1, 2, 3$) is the usual relativistic momentum flux-density tensor. In the reference frame comoving with the front of the Poynting jet, a Lorentz transformation gives $T'_{zz} = \Gamma^2[T_{zz} - 2(V_z/c)T_{0z} + (V_z/c)^2 T_{00}]$, where $T_{zz} = (E_r^2 + B_\phi^2 - B_z^2)/8\pi = B_z^2(4\Gamma^2 - 3)/8\pi$ (where the last equality uses our expressions for the fields). Furthermore, $T_{0z} = E_r B_\phi/4\pi = B_z^2[4\Gamma(\Gamma^2 - 1)^{1/2}]/8\pi$, and $T_{00} = (E_r^2 + B_\phi^2 + B_z^2)/8\pi = B_z^2(4\Gamma^2 - 1)/8\pi$. Combining these equations gives $T'_{zz} = B_z^2/8\pi$. Since T'_{zz} varies with radius, we take its average between r_1 and r_2 , which gives $\langle T'_{zz} \rangle = B_0^2/[8\pi\bar{\mathcal{R}}^2(\Gamma^2 - 1)^2]$, assuming $r_1 \ll r_2$.

In the reference frame comoving with the head of the jet, force balance implies that the ram pressure of the external ambient medium $\rho_{\text{ext}}\Gamma^2 V_z^2$ is equal to $\langle T'_{zz} \rangle$. This assumes that V_z is much larger than the sound speed in the external medium; however, details of the shock(s) at the jet front are not considered here. Thus, we have $(\Gamma^2 - 1)^3 = B_0^2/(8\pi\bar{\mathcal{R}}^2\rho_{\text{ext}}c^2)$. For $\Gamma \gg 1$,

$$\Gamma \approx 8 \left(\frac{10}{\bar{\mathcal{R}}}\right)^{1/3} \left(\frac{B_0}{10^3 \text{ G}}\right)^{1/3} \left(\frac{1 \text{ cm}^{-3}}{n_{\text{ext}}}\right)^{1/6}, \quad (6)$$

where $n_{\text{ext}} = \rho_{\text{ext}}/\bar{m}$, with being \bar{m} the mean particle mass. A necessary condition for the validity of equation (6) is that the axial speed of the counterpropagating fast magnetosonic wave (in the lab frame) be larger than V_z so that ‘‘information’’ (the field twist) can propagate in both directions along the jet. This condition can be expressed as $\Gamma^2 < v'_A/2$, where $v'_A \equiv |\mathbf{B}'|/(4\pi\rho')^{1/2}$ is the Alfvén speed in the comoving frame of the jet. The above-mentioned force-free condition is $(v'_A)^2 \gg 1$. The other important condition is that $\bar{\mathcal{R}}^2 = (r_0/r_g)^2 \gg 1$, so that the jet energy is extracted mainly from the disk (rather than from the rotating black hole).

The derived value of Γ is on the order of the Lorentz factors of the expansion of parsec-scale extragalactic radio jets observed with very long baseline interferometry (see, e.g., Zensus et al. 1998). This interpretation assumes that the radiating electrons (and/or positrons) are accelerated to high Lorentz factors ($\gamma \sim 10^3$) at the jet front and move with a bulk Lorentz factor Γ relative to the observer. The luminosity of the $+z$ Poynting jet is $\dot{E}_j = c \int_0^2 r dr E_r B_\phi/2 = c B_0^2 \bar{\mathcal{R}} r_g^2/3 \approx 2.2 \times 10^{45} (B_0/10^3 \text{ G})^2 (\bar{\mathcal{R}}/10) (M/10^9 M_\odot)^2 \text{ ergs s}^{-1}$, where M is the mass of the black hole.

The region of the collimated field of the Poynting jet may be kink-unstable. The instability will lead to a helical distortion of the jet, with the helix having the same twist about the z -

axis as the axisymmetric \mathbf{B} -field. A relativistic perturbation analysis is required, including the displacement current. The evolution of the jet evidently depends on *both* the speed of the propagation of the lateral displacement and the velocity of the propagation of the “head” of the jet V_z . Relativistic propagation of the jet’s head may act to limit the amplitude of the helical kink distortion of the jet.

For long timescales, the Poynting jet is of course time-dependent because of the angular momentum it extracts from the inner disk ($r < r_0$), which in turn causes r_0 to decrease with time (L02). This loss of angular momentum leads to a “global magnetic instability,” the collapse of the inner disk (Lovelace, Romanova, & Newman 1994; Lovelace, Newman, & Roma-

nova 1997; L02), and a corresponding outburst of energy in the jets from the two sides of the disk. Such outbursts may explain the flares of active galactic nucleus blazar sources (Romanova & Lovelace 1997; Levinson 1998) and the one-time outbursts of gamma-ray burst sources (Katz 1997).

We thank an anonymous referee for helping to improve this work and Hui Li and Stirling Colgate for valuable discussions. This work was supported in part by NASA grants NAG5-9047 and NAG5-9735, by NSF grant AST 99-86936, and by DOE cooperative agreement DE-FC03-02NA00057. M. M. R. received partial support from NSF POWRE grant AST 99-73366.

REFERENCES

- Bisnovatyi-Kogan, G. S., & Lovelace, R. V. E. 2001, *NewA Rev.*, 45, 663
 Bridle, A. H., & Eilek, J. A., eds. 1984, in *Physics of Energy Transport in Extragalactic Radio Sources* (Greenbank: NRAO)
 Bührke, T., Mundt, R., & Ray, T. P. 1988, *A&A*, 200, 99
 Colgate, S. A., Li, H., & Pariev, V. I. 2001, in *AIP Conf. Proc.* 586, 20th Texas Symp. on Relativistic Astrophysics, ed. J. C. Wheeler & H. Martel (Melville: AIP), 259
 Eikenberry, S., Matthews, K., Morgan, E. H., Remillard, R. A., & Nelson, R. W. 1998, *ApJ*, 494, L61
 Gold, T., & Hoyle, F. 1960, *MNRAS*, 120, 89
 Katz, J. I. 1997, *ApJ*, 490, 633
 Levinson, A. 1998, *ApJ*, 507, 145
 Li, H., Lovelace, R. V. E., Finn, J. M., & Colgate, S. A. 2001, *ApJ*, 561, 915
 Lovelace, R. V. E., Li, H., Koldoba, A. V., Ustyugova, G. V., & Romanova, M. M. 2002, *ApJ*, 572, 445 (L02)
 Lovelace, R. V. E., Newman, W. I., & Romanova, M. M. 1997, *ApJ*, 484, 628
 Lovelace, R. V. E., Romanova, M. M., & Newman, W. I. 1994, *ApJ*, 437, 136
 Lovelace, R. V. E., Wang, J. C. L., & Sulkanen, M. E. 1987, *ApJ*, 315, 504
 Lynden-Bell, D. 1996, *MNRAS*, 279, 389
 ———. 2003, *MNRAS*, 341, 1360
 Meier, D. L., Koide, S., & Uchida, Y. 2001, *Science*, 291, 84
 Mirabel, I. F., & Rodríguez, L. F. 1994, *Nature*, 371, 46
 Mundt, R. 1985, in *Protostars and Planets II*, ed. D. C. Black & M. S. Mathews. (Tucson: Univ. Arizona Press), 414
 Newman, W. I., Newman, A. L., & Lovelace, R. V. E. 1992, *ApJ*, 392, 622
 Romanova, M. M., & Lovelace, R. V. E. 1997, *ApJ*, 475, 97
 Romanova, M. M., Ustyugova, G. V., Koldoba, A. V., Chechetkin, V. M., & Lovelace, R. V. E. 1998, *ApJ*, 500, 703
 Scharlemann, E. T., & Wagoner, R. V. 1973, *ApJ*, 182, 951
 Ustyugova, G. V., Lovelace, R. V. E., Romanova, M. M., Li, H., & Colgate, S. A. 2000, *ApJ*, 541, L21
 Zensus, J. A., Taylor, G. B., & Wrobel, J. M., eds. 1998, *IAU Colloq.* 164, *Radio Emission from Galactic and Extragalactic Compact Sources* (ASP Conf. Ser. 144; San Francisco: ASP)